Thermal compensation system comissioning for O3 and a study of the the Pockels effect of an AlGaAs coating

Syracuse University

Daniel Vander-Hyde

October 27, 2021

Abstract

Abstract goes here

Dedication

Declaration

I declare that

Acknowledgements

Contents

Chapter 1

Introduction

Chapter 2

TCS comissioning for O3

As shown in Chapter 1, increasing input power directly relates to an interferometer's sensitivity to detecting gravitational waves. This comes with a few implications, but one in particular is the necessity for thermal compensation. As the interferometer increases input power, you directly couple more light into the Fabry-Pérot cavity arms. The optics, even with super low absorption ($\approx$ 400 ppb) still induce thermo-optic effects with the projected circulating arm power of 200 kW. A symptom of this is mode mismatching throughout the interferometer, a problem that contributes to loss of optical power at the anti-symmetric port which can reduce sensitivity two-fold: loss of power to your readout and reduced efficacy of implementing quantum squeezing.

2.0.1 TCS preloading for O3

Reference to TVO's thesis for preloading settings based on his model[1]

2.0.2 Point absorbers

Coupling into control signals (ASC and LSC)

- Loss of interferometer control
- Reported in "TCS comissioning for O3" @ LVK, I reference a Craig elog where he reports loss of sideband power after thermalization (particularly POP LF, REFL LF, POP 18, POP 45)
- A. Brooks explains in [2]

2.0.3 RH input conditioning

Some notes about the analytical calculations of RH (There is a paper on this). Notes as to why this 12 hour time constant is not optimal for thermal compensation.

2.1 Optimizing thermo-optic response

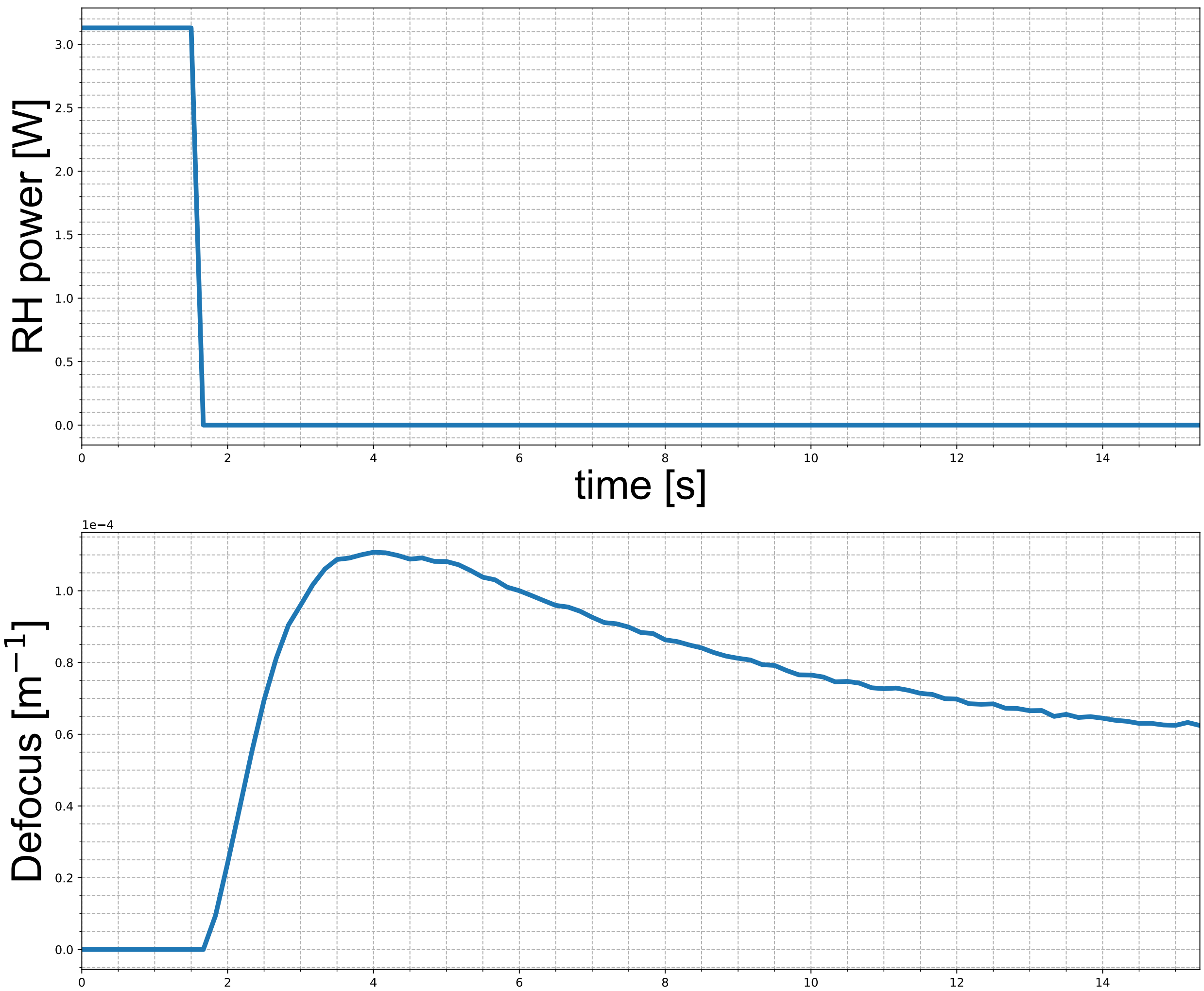

Figure 2.1: ITMY thermo-optic response to a 3.13 Watt power reduction to ring heaters. It's after ≈ 12 hours after the change was made do you start to see a small enough $\frac{d\alpha_{sp}}{dt}$ when you can assume a steady thermal lens.

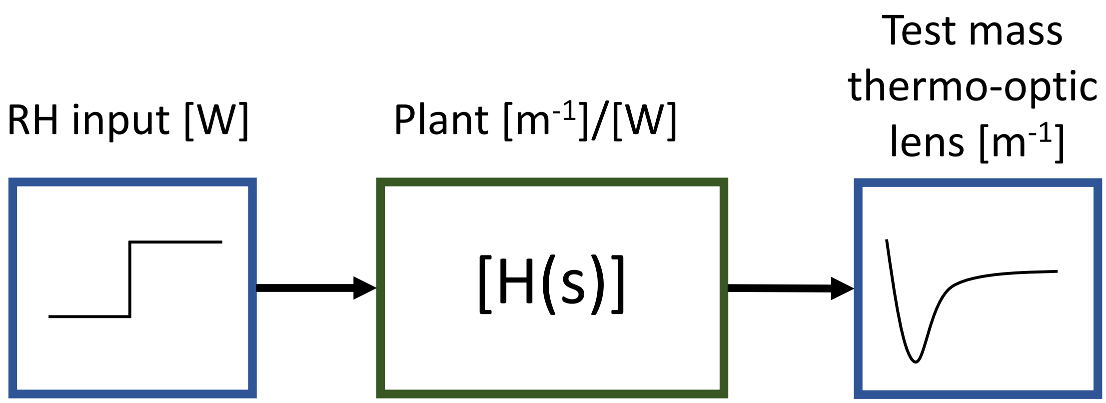

Figure 2.2: A pictograph showing how the plant transforms the signal. The example of this can be seen in Fig [2.1]

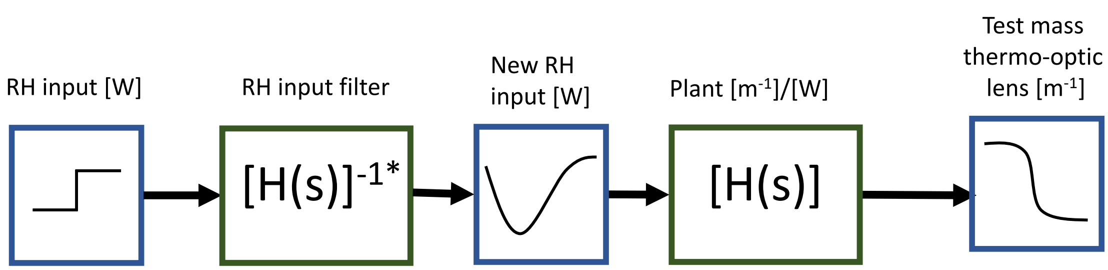

Figure 2.3: A pictograph showing the system with real time digital filtering for an improved thermo-optic response. The RH input filter is created by inverting the plant filter combine with a low pass and added poles to the zpk model to ensure stability.

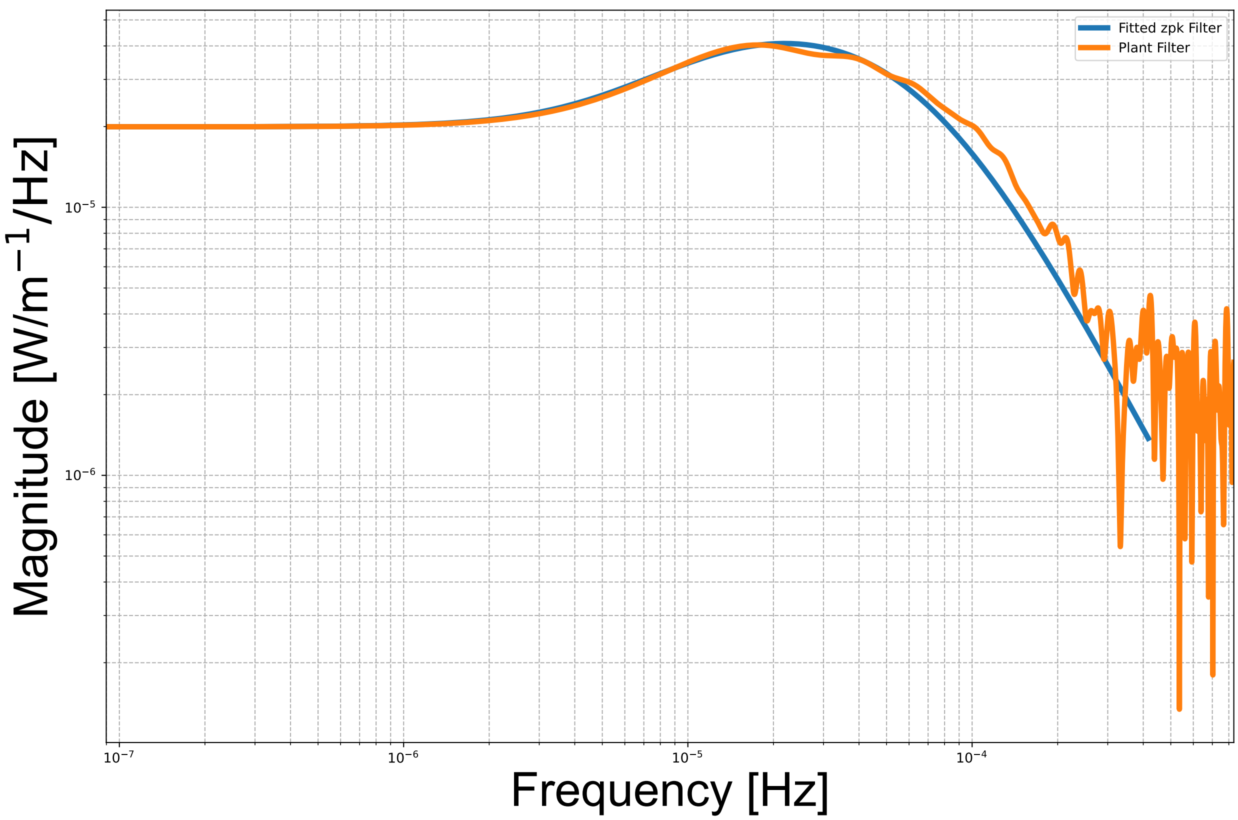

Figure 2.4: Showing the PSD of the RH response (normalized by the input RH power) over a an $\approx$ 12.5 hour period. The zpk model of the fitted filter (H(s)) is $9.2545e-12\frac{(s+3.14210e-5)}{(s+8.168e-5)(s+0.0003142)(s+0.0005969)}$

2.2 Dynamic Thermal compensation

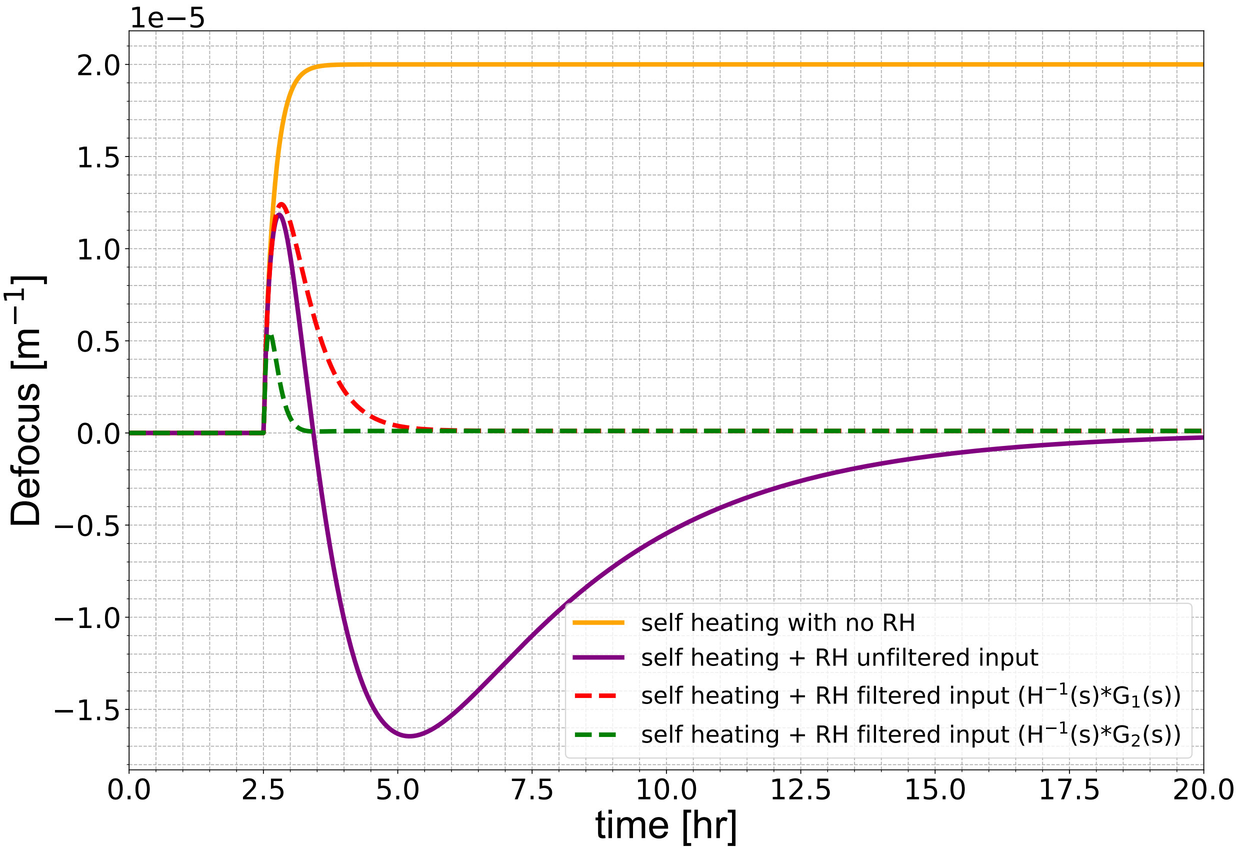

Figure 2.5: Comparison of the natural RH response and the response to the conditioned input. The above plot is simulated in Matlab by passing the RH input time series (top plot) through the $[H(s)]^{-1*}$ and $H(s)$ to acquire with the result lensing behavior on the bottom plot.

Analytical expression of self heating from beam [3]

2.3 Limitations

Chapter 3

Electro-optic study of an AlGaAs coated sample

As mentioned in Section (1?) one of the many LIGO fundamental noise sources is coating thermal noise from the $SiO_2 - TaO_5$ ALIGO coating. As ALIGO approaches its designed sensitivity various coating solutions are currently proposed to mitigate thermal noise coupling into the detector output. With the potential to reduce noise by a factor of 5, AlGaAs shows much promise with next generation detectors, though with different material properties of this crystalline coating introduces new coating noise couplings. A notable source of noise is the linear electro-optic property of the crystal (dn/dE), also known as the Pockels effect. Characterizing currently proposed AlGaAs coated "witness" samples thorough extensive analysis and experimental data of the aforementioned properties is essential for the use of AlGaAs in gravitational wave interferometers. The following section dedicated to the discussion of said properties starting with the fundamentals on the Pockels effect, the coupling mechanism and estimates of coupling.

3.0.1 The Pockels Effect

This property of anisotropic crystalline media (ACM) explains the depdendence of the index of refraction of a material with a relatively slowly varying (with respect to the EM radiation) Electric field . This property of ACM is what allows electro-optic modulators to operate as light phase modulators[4] [5]. More to be discussed: How the modulation of the phase of the carrier field is dependent on the orientation of its wave vector with respect to the crystal structure, the modulating electric field direction and strength, (other items to discuss in terms of introducing the effect)

3.1 Phase modulation of light propogating through stratified anisotropic crystalline media

3.1.1 Coating parameters

Info from Steve: λ / 4 stack. It is 36 layers of GaAs interspersed with 35 layers of AlGaAs. GaAs forms the top and bottom layer to protect the AlGaAs from absorbing oxygen from the air. High Index: GaAs, n=3.480, layer thickness is 76.43 nm Low Index: $Al_{0.92}Ga_{0.08}As$, n=2.977, layer thickness is 89.35 nm

3.1.2 Fejer and Bonilla approach

Fejer and Bonilla take an analytical approximation approach when finding the impact of the Electric field to the change in phase of the light through a crystalline anisotropic media.

3.1.3 Ballmer approach

3.2 Projected DARM coupling

3.3 Experiment

3.3.1 Design

Short in-air cavity with a PDH lock.

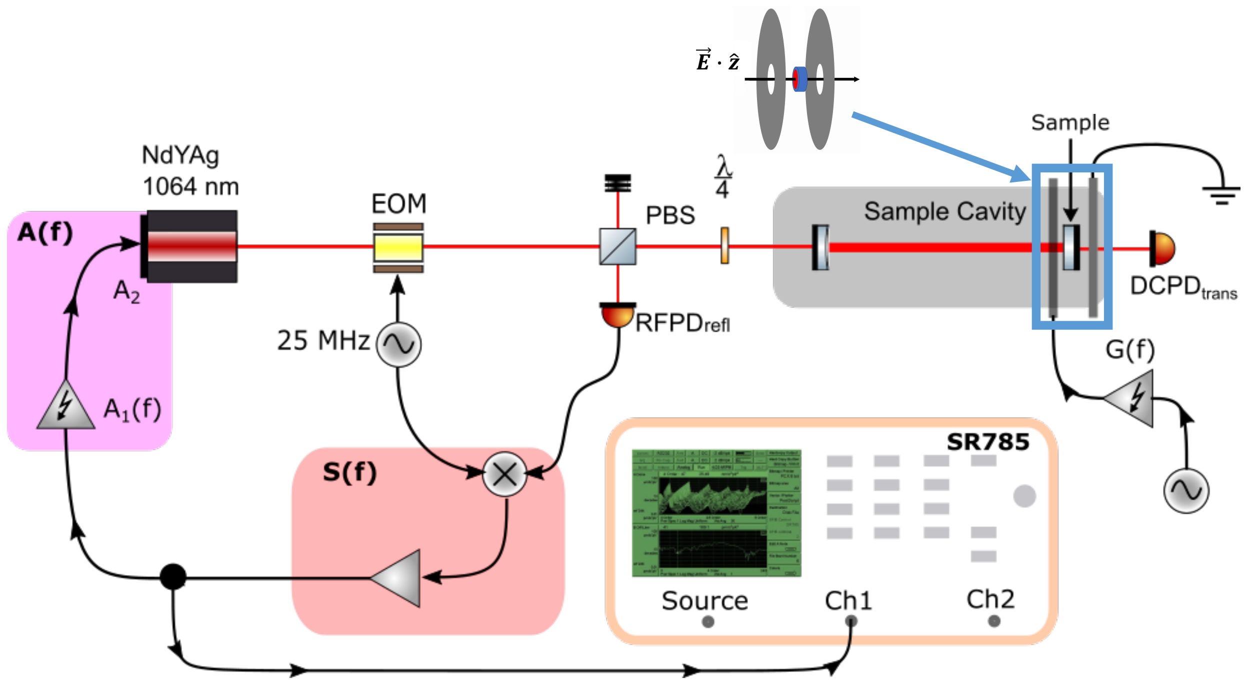

Figure 3.1: Experiment schematic. Needs to be updated with the Agilent 4395A analyzer.

Maximizing the electric field normal to the sample coating ($|E_z|$) within the coating. Given a chosen aperture size (established by choosing the an aperture size that is 5 times larger than the beam size). An optical mount for the sample made with MACOR, along with glass bearnings and a McMaster-Carr 8-32, 1/2" ceramic screw were used to There are two relevant configurations of this experiment: 1) an all-in-one MACOR assembly where the electrodes are mechanically coupled to the optical mount, and 2) larger mechanically decoupled electrode plates.

3.3.2 $|E_z|$ strength

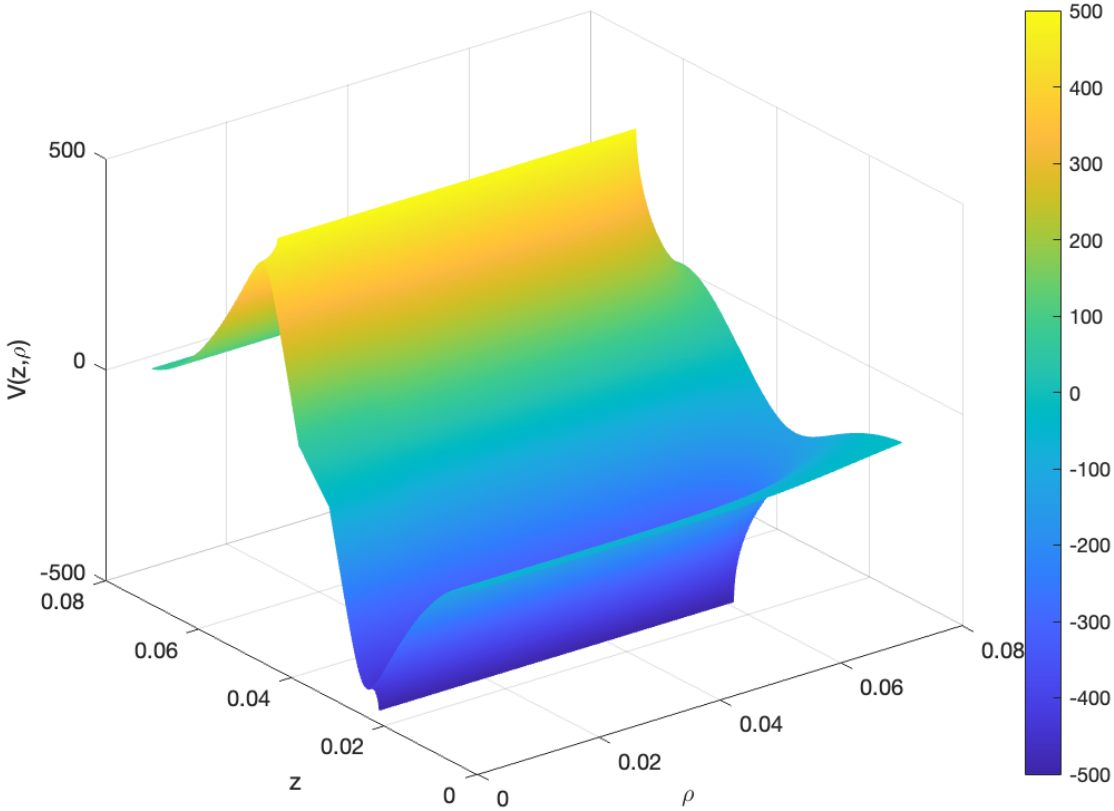

Figure 3.2: Poisson calculator output potential map ($V(z, \rho)$)

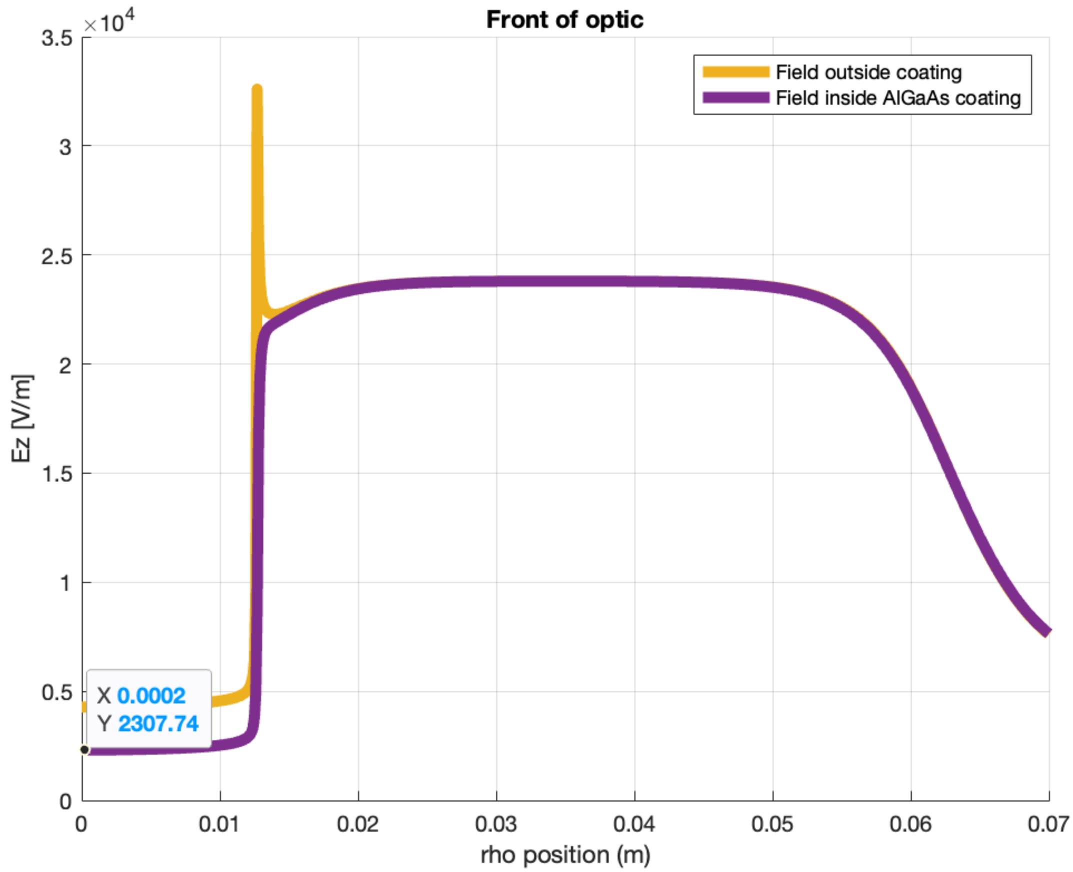

Figure 3.3: $|E_z|$ screened by coating and $|E_z|$ immediately outside AlGaAs coating

TREK 10/10B-HS HVA frequency depdendent measurement. Using Poisson calculator to estimate field strength within coating

3.3.3 Calibration

$V_{\mathrm{FSSOUT}} \rightarrow m_{\mathrm{rms}}/\sqrt{\mathrm{Hz}}$

$$\Delta L = \mathrm{source} * \alpha(f)A(f) * \frac{1 + OLG(f)}{OLG(f)} * \frac{L_{\mathrm{cav}}}{f_{\mathrm{laser}}}$$

3.3.4 Noise Floor

3.3.5 Drive coupling

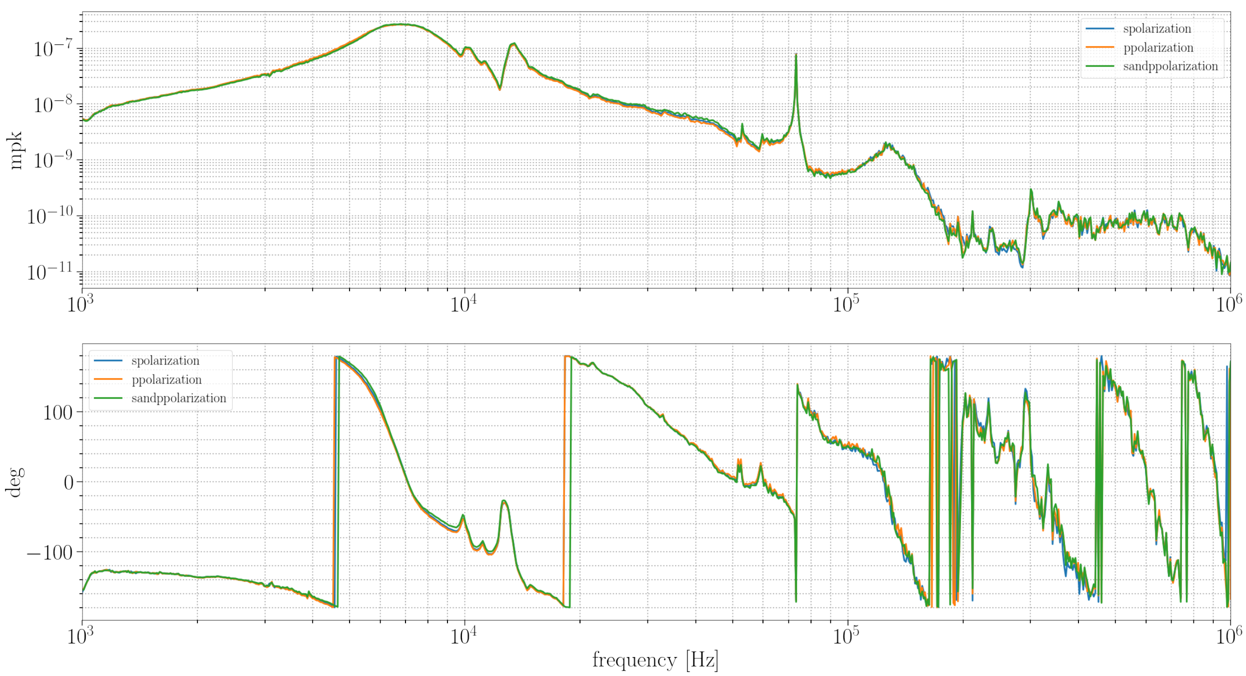

Figure 3.4: Figure that will include the displacement noise floor, (pockels estimate)*(poisson calculator estimate)*(HVA drive frequency dependence), and the drive coupled measurement figure size needs to be increased

Mechanical modes

Sample and mount mechanical mode excitations. Seen with both AlGaAs and a HR coating from an AtFilm (IBS coating)

Vibration of plates (Leissa) Computing frequency and order of magnitude

Steve's COMSOL model

Chapter 4

Conclusion

Chapter 5

Appendix

5.1 Calibration math for Electro-optic effect

The frequency response measurement shown in (?) records the following transfer function in dB of the following:

$$\alpha(f) = \frac{CH2(f)}{Source}$$

Channel

We also know that the error signal spectra of the loop is probed by $CH2(f)$:

$$CH2(f) = \frac{\mathrm{S}(f) * signal_V}{(1 - \mathrm{OLG}(f))}$$

Where $signal_V$ is the uncalibrated voltage output from the mixer, $\mathrm{S}(f)$ is the FSS transfer function, and $\mathrm{OLG}(f)$ is the open loop gain of the PDH system.

5.2 Poisson calculator / code

5.3 MACOR assembly

References

[1] T. Vo, *Adaptive Mode Matching in Advanced LIGO and beyond.* PhD thesis, Syracuse NY, 2019.

[2] A. Brooks *et al.*, "Point absorbers in advanced ligo," *Optical Scoiety of America*, vol. 60, pp. 4047–4063, 2021.

[3] P. Hello and J.-Y. Vinet, "Analytical models of thermal aberrations in massive mirrors heated by high power laser beams," *Journal de Physique*, vol. 51, pp. 1267–1282, 1990.

[4] A. Yariv, *Quantum Electronics (3rd. ed).* John Wiley & Sons, 1989.

[5] J. F. Nye, *Physical properties of crystals (Their representation by tensors and matrices).* Oxford University Press, 1985.